Impact of uptake time on image quality of [^{68}Ga]Ga-PSMA-11 PET/CT

Esmée C. A. van der Sar[1] | Sebastiaan L. Meyer Viol[1,2] |

Arthur J. A. T. Braat[1] | Rob van Rooij[1] | Marnix G. E. H. Lam[1] |

Hugo W. A. M. de Jong[1] | Bart de Keizer[1]

[1]Department of Radiology and Nuclear Medicine, University Medical Center Utrecht, Utrecht, The Netherlands

[2]Department of Radiology and Nuclear Medicine, Amsterdam University Medical Center, Amsterdam, The Netherlands

Correspondence
Esmée C.A. van der Sar, Department of Radiology and Nuclear Medicine, University Medical Center Utrecht, Heidelberglaan 100, 3584 CX Utrecht, The Netherlands.
Email: e.c.a.vandersar@umcutrecht.nl

Esmée C. A. van der Sar and Sebastiaan L. Meyer Viol share first authorship.

Abstract

Background: With the introduction of prostate specific membrane antigen (PSMA) PET/CT, the detection rate of prostate cancer metastases has improved significantly, both for primary staging and for biochemical recurrence. EANM/SNMMI guidelines recommend a 60 min time interval between [^{68}Ga]Ga-PSMA administration and acquisition.

Purpose: This study evaluates the possibility of a shorter time interval by investigating the dynamic change in image quality measures.

Method: We retrospectively analyzed 10 consecutive prostate cancer patients who underwent a dynamic whole body [^{68}Ga]Ga-PSMA-11 PET/CT of 75 min from skull vertex to mid-thigh using Siemens FlowMotion. PET images were acquired directly after injection of 1.5 MBq/kg [^{68}Ga]Ga-PSMA-11. Image quality measures included lesion maximum standardized uptake value corrected for lean body mass (SUL$_{max}$), tumor-to-background ratio (TBR), and contrast-to-noise ratio (CNR). Quantitative analysis of image quality in dynamic PET was performed using PMOD (version 4.2). Regions of interest (ROIs), drawn included different types of prostate lesions (primary tumor, lymph nodes, and bone metastasis), organ tissue (liver, spleen, lacrimal gland, submandibular gland, parotid gland, urinary bladder, kidneys blood pool [ascending aorta], left ventricle), bone tissue (4th lumbar vertebral body [L4]) and muscle tissue (gluteus maximus). To further investigate image quality four 10 min multi-frame reconstructions with clinical parameters were made at different post-injection times (15, 30, 45, and 60 min). A nuclear medicine physician performed a blinded lesion detectability evaluation on these multi-frame reconstructions for different prostate cancer lesions.

Results: Six primary prostate tumors in seven patients with prostate in situ, 13 lymph node metastases in six patients and up to 12 bone metastases in three patients were found. The different prostate lesion types (lymph nodes metastases, bone metastases, and primary prostate tumor) all show an increase in average SUL$_{max}$, TBR, and CNR over time during the scan. The normalized average SUL$_{max}$, TBR, and CNR of the combined prostate lesions at 15, 30, and 45 min post-injection scans were all significant $p < 0.05$ lower from the 60 min post-injection [^{68}Ga]Ga-PSMA-11 PET/CT (9.5 ± 4.5, 12.7 ± 6.2, and 41.8 ± 24.5, respectively). At patient level, the reader concluded the same regarding the presence/absence of primary prostate cancer recurrence, lymph node metastases, and/or bone metastases on all <60 min post-injection

[^{68}Ga]Ga-PSMA-11 PET/CT's in comparison to the reference scan (60 min post-injection). At lesion level, all bone metastases seen on the reference scan were also seen on all <60 min post-injection [^{68}Ga]Ga-PSMA-11 PET/CT's but there were some lymph nodes ($n = 2$) metastases missed on the 15, 30, and 45 min post-injection scans. One lymph node metastasis on both the 15 and 30 min post-injection [^{68}Ga]Ga-PSMA-11 PET/CT's was missed and one lymph node metastasis was missed, only on the 45 min post-injection [^{68}Ga]Ga-PSMA-11 PET/CT.

Conclusion: Shorter post-injection times (15, 30, and 45 min) compared to the recommended post-injection time of 60 min are not optimal. However, the impact of a shorter time interval of 45 min instead of 60 min between [^{68}Ga]Ga-PSMA-11 administration and the start of PET/CT acquisition on both image quality (SUL_{max}, TBR, and CNR) and lesion detection, while significant, is small.

KEYWORDS

dynamic PSMA PET/CT, prostate cancer, uptake time

1 | INTRODUCTION

Since the introduction of prostate specific membrane antigen (PSMA) PET/CT, the detection rate of prostate cancer metastases has improved significantly, both for primary staging and for biochemical recurrence.[1–3] As a result PSMA PET/CT is rapidly being included in international prostate cancer protocols.[4] The current EANM/SNMMI guideline recommends a 60 min time interval (also known as uptake time) between [^{68}Ga]Ga-PSMA administration and scan acquisition.[5] This recommendation is based on one study evaluating the biodistribution of [^{68}Ga]Ga-PSMA-11 after 60 and 180 min.[6] Other time intervals were not investigated in this study. A shorter time interval between [^{68}Ga]Ga-PSMA administration and scan acquisition may offer benefits. These benefits include a shorter waiting time for patients, a higher scanning rate, and a higher activity of [^{68}Ga]Ga-PSMA-11 as the half-life of [^{68}Ga]Ga-PSMA-11 is 68 min. Even if there are no differences in image quality between different time intervals, there may still be a benefit of a more flexible time window between [^{68}Ga]Ga-PSMA administration and scan acquisition. A potential downside of a shorter time interval between [^{68}Ga]Ga-PSMA administration and scan acquisition is that there is less uptake in the lesions, while the activity in normal organs and background is still higher.[7] The effect of a shorter uptake time on image quality is still unknown.

One study proposed that PSMA PET/CT could be performed at 35−59 min post-injection by investigating the difference in mean and maximum standard uptake values ($SUV_{mean/max}$).[7] While this result is promising, important measures of image quality: tumor-to-background ratio (TBR), and contrast-to-noise ratio (CNR) were missing, as a high lesion SUV does not automatically indicate a better distinction between tumor and background. Furthermore, a lesion detectability analysis was only performed between 6 and 60 min. Therefore further investigation is needed to determine image quality of [^{68}Ga]Ga-PSMA-11 PET/CT at different uptake times.

This study aims to evaluate the possibility of a shorter time interval between [^{68}Ga]Ga-PSMA-11 administration and the start of PET/CT acquisition by analyzing the development of image quality measures $SUV_{mean/max}$, TBR, and CNR over time and investigating lesion detectability of reconstructions at different time frames.

2 | METHODS

2.1 | Participants

A total of 10 consecutive prostate cancer patients who were referred to our department for a [^{68}Ga]Ga-PSMA-11 PET/CT underwent a dynamic [^{68}Ga]Ga-PSMA-11 PET/CT. This was part of a prospective pilot study between October 2020 and November 2021. Image data were retrospectively analyzed. Patients were imaged for either primary staging of prostate cancer ($n = 1$), follow-up ($n = 2$), biochemical recurrence ($n = 5$), or (biochemical) progression ($n = 2$). This study followed the principles of the Declaration of Helsinki and its subsequent amendments. Need for informed consent was waived by the institutional medical ethics committee (METC number 18-872).

2.2 | Radiopharmaceutical

[^{68}Ga]Ga-PSMA-11 was prepared using a GMP-grade ^{68}Ge/^{68}Ga generator and a semi-automated synthesis module (Eckert & Ziegler, Berlin, Germany and ITG, Munich, Germany). Each synthesis was performed following the manufacturer's instructions using PSMA-11 ligand (ABX, Radeberg, Germany).
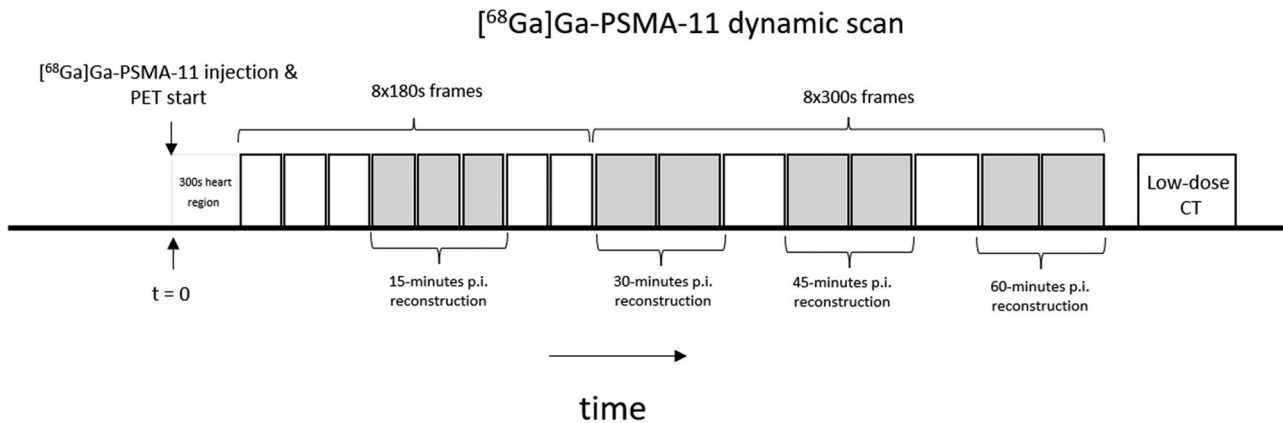
FIGURE 1 Dynamic image acquisition protocol. The 8×180 s frames, and 8×300 s frames are used for analysis of mean and maximum standardized uptake values corrected for lean body mass ($SUL_{mean/max}$) and tumor-to-background ratio (TBR), while the multi-frame reconstructions (in grey) are used for lesion detectability, $SUL_{mean/max}$, TBR, and contrast-to-noise ratio (CNR) analysis.

2.3 | Injection, dynamic acquisition, and reconstruction

Dynamic scans were performed using a Siemens Biograph Vision 600 (axial field of view (FOV) = 26.3 cm). All patients were asked to void urine directly before the start of the scan. A total of 1.5 MBq/kg [^{68}Ga]Ga-PSMA-11 was administered intravenously on the scan table, followed by 500 mL saline.

PET images were acquired directly after injection. Patients underwent a scan of 75 min from skull vertex to mid-thigh using Siemens FlowMotion. Siemens FlowMotion enables dynamic acquisition over the entire scan range by continuously moving the patient in the axial orientation with a defined number of passes. Dynamic acquisition started with a 6 min acquisition of the heart region to enable pharmacokinetic modelling on this data set (this 6 min frame will not be used in this study). Thereafter eight whole-body passes of 3 min and eight whole-body passes of 5 min were scanned (Figure 1). After each whole-body pass the patient was moved back in 20 s to starting position. A low dose CT was acquired immediately after PET imaging for attenuation correction and anatomical mapping (120 ref. kv, 40 ref. mAs).

Images were reconstructed with an iterative algorithm with four iterations and five subsets (4i5s), including time-of-flight (TOF), point spread function (PSF) modelling, and no filter. Standardized uptake values (SUV) were corrected for lean body mass (SUL),[8] as for quantitative analysis it was shown that the lean body mass correction is preferable over body weight correction.[9] For dynamic image analysis of image quality measures, each whole-body pass was reconstructed as a separate frame. This results in eight frames of 3 min and eight frames of 5 min (Figure 1).

In addition, to investigate lesion detectability and image quality measures, four 10 min multi-frame reconstructions were made at different time points with reconstruction parameters used in clinic (PSF + TOF, 4i5s, 4 mm Gauss filter). These reconstruction were made at 15–24, 30–40, 45–55, and 60–70 min post-injection (Figure 1). Due to the acquisition protocol, the multi-frame reconstruction of the 15 min post-injection is only 9 min. Hereafter these four multi-frame reconstructions with clinical parameters will be referred to as the "clinical scans/reconstructions."

2.4 | Delineation

Quantitative analysis of dynamic PET was performed using PMOD (version 4.2). Regions of interest (ROIs) drawn included different type of prostate lesions (primary tumor, lymph nodes, and bone metastasis), organ tissue (liver, spleen, lacrimal gland, submandibular gland, parotid gland, urinary bladder, kidneys, blood pool [ascending aorta], left ventricle), bone tissue (4th lumbar vertebral body [L4]) and muscle tissue (gluteus maximus). Volumes of interest (VOIs) (10–20 mm sized sphere) in organs with homogeneous uptake were drawn within organ boundaries. For delineation of bladder and kidneys, a region growing algorithm at organ boundaries was used.

2.5 | Image quality measures

For each frame and each clinical reconstruction of the dynamic scan, SUL_{max} of tumor lesions, and SUL_{mean} of organs and background tissue was calculated. In addition for each frame and clinical reconstruction the TBR of tumor lesions was calculated. TBR was defined as:

$$TBR = \frac{\text{Lesion } SUL_{max}}{\text{Background } SUL_{mean}} \quad (1)$$

For lymph node metastases and recurrent primary prostate tumors, the blood pool in the left ventricle was

used as a background measure. For bone metastases activity in bone marrow of the fourth lumbar vertebral body was used as a background measure.

In addition, CNR was calculated. CNR is defined as[10]:

$$CNR = \frac{\text{Lesion } SUL_{max} - \text{Background } SUL_{mean}}{\sigma_{background}}, \quad (2)$$

With $\sigma_{background}$ the standard deviation of the background VOI. The background VOI was drawn in a homogenous region to avoid deviations inside the VOI which are not the result of noise. As the short and varying (3 and 5 min) frame duration in the dynamic scan would have impact on the noise measure, the CNR was calculated only on the clinical 10 min reconstructions at 15, 30, 45, and 60 min.

The results show the average $SUL_{max/mean}$, TBR, and CNR over all patients for each multi-frame reconstruction. If a patient contained multiple lesions of one type, an average result of the lesions for that patient was calculated first. No additional weighting was applied, to avoid bias towards patients with a high number of lesions.

2.6 | Generation of dynamic image quality curves

Non-linear least squares polynomial fits of $SUL_{max/mean}$ and TBR were made in Python (v3.9) for trend visualization. The order of the fit was either first, second, or third, based upon least-squares error, and randomness of residual error, while avoiding over-fitting. To estimate the standard deviation of the fit, a Monte Carlo simulation with $n = 1000$ was performed on the polynomial fit. Hereby the assumption was made that the standard deviation of the fitting parameters is Gaussian distributed.

2.7 | Clinical scans image quality comparison

Data of the clinical scans are presented as mean $\pm$ standard deviation (SD). To compare the clinical scans between patients all image quality measures were normalized on a lesion level by the 60 min post-injection [68Ga]Ga-PSMA-11 PET/CT.

The normalized patient average SUL_{max}, TBR, and CNR of the lesions in the four clinical scans were compared by a paired two sided t-test using IBM SPSS statistics 26.0.0.1. A p-value < 0.05 was considered significant. The statistical t-test analysis was performed on the total set of lesions and not on sub-sets (primary tumor, lymph nodes, and bone metastasis). This was done to create one general outcome measure, while

TABLE 1 Baseline patients characteristics.

Characteristic	Value
Total patients, number	10
Detected lesions:	
Local recurrence	Six, in seven patients
Lymph node metastases	13, in six patients
Bone metastases	>12 in three patients
Age, years (median, IQR)	73 (66–76)
Baseline PSA, ng/mL (median, IQR)	5.15 (2.75–15.18)
Gleason-score: number of patients (%)	
7	6 (60%)
8	2 (20%)
9	1 (10%)
Not reported	1 (10%)
Prior therapy: number of patients (%)	
Surgical resection of primary tumor	3 (30%)
Radiotherapy	7 (70%)
Docetaxel and/or cabazitaxel	1 (10%)
Abiraterone and/or enzalutamide	3 (3%)
Radioligand therapy ([223Ra]Ra-dichloride, [177Lu]Lu-PSMA-617)	2 (20%)
Injected dose, MBq/Kg (mean, SD)	1.57 (0.09)

Abbreviations: ECOG, Eastern Cooperative Oncology Group; IQR, Inter quartile range; Lu, Lutetium; PSA, Prostate specific antigen; PSMA, Prostate specific membrane antigen; Ra, Radium; SD, Standard deviation.

also ensuring the data size was large enough for the statistical test.

2.8 | Lesion detectability evaluation

The four (anonymized) clinical [68Ga]Ga-PSMA-11 PET/CT reconstructions (15–24, 30–40, 45–55, and 60–70 min post-injection) were retrospectively evaluated by an experienced nuclear medicine physician (16 years of experience) on primary prostate cancer recurrence yes/no and bone- and lymph node metastases using a 5-point Likert scale score (benign, probably benign, indecisive, probably malign, malign). A score of ≥ 3 was considered positive. The 60 min post-injection [68Ga]Ga-PSMA-11 PET/CT was considered the reference for true and false positive lesions.

3 | RESULTS

A total of 10 patients were included. Patient characteristics are shown in Table 1. Six primary prostate tumors in seven patients with prostate in situ were found. Furthermore, 13 lymph node metastases were found in six
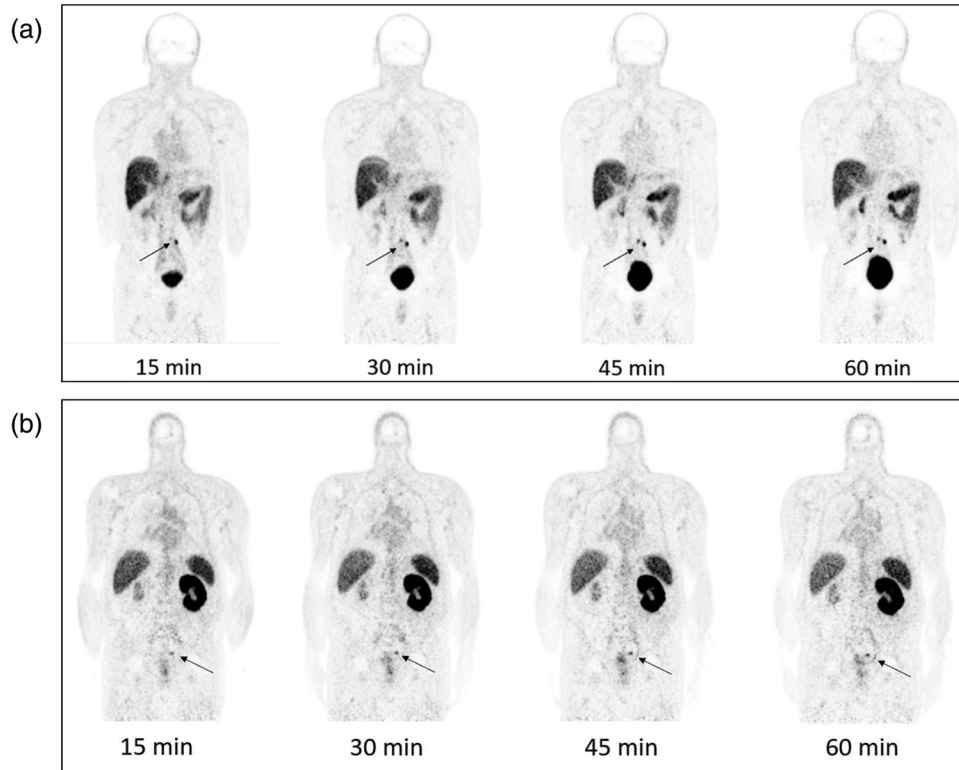
FIGURE 2 Clinical reconstructions at different time-points post-injection in minutes (min) of two different patients. The lymph node metastases are indicated with an arrow. (a) Represents a patient with two lymph node metastases with high maximal standardized uptake values corrected for lean body mass (SUL_{max}). The SUL_{max} increases from 7.21 to 9.65 and from 10.68 to 12.42, respectively, depending on scan time. (b) Represents a patient with a lymph node metastases with low SUL_{max}. The SUL_{max} increases from 3.15 to 5.03.

patients, two patients had one bone metastasis and one patient had multifocal bone metastases, in this patient we delineated 10 metastases. Two representative visual examples of dynamic [^{68}Ga]Ga-PSMA-11 PET imaging at different time points post-injection can be found in Figure 2.

3.1 | Normal organ time-activity curves

Average time-activity curves of organs are shown in Figure 3. Uptake of left/right kidney, urinary bladder, parotid-, submandibular-, and lacrimal-glands increased over time. While most organs showed a sharper increase in activity post-injection the curves flatten out after approximately 45 min. Uptake by the spleen and liver decreased over time. This pattern was similar for all individual patients.

3.2 | Background tissue

All background tissues (blood pool in ascending aorta, L4, gluteal muscle, and left ventricle) showed a sharp decrease in average SUL_{mean} the first 30−45 min

post-injection, after which the decrease flattened out (Figure 4).

3.3 | Pathological lesions SUL_{max}

The different prostate lesion types (lymph nodes metastases, bone metastases, and primary prostate tumor) all show an increase in average SUL_{max} over time during the scan (Figure 5a). The increase in average SUL_{max} is more steep at first and flattens off. Based on the fit average SUL_{max} of lymph nodes increases from 6.74 at 7.5 min post-injection to 11.13 at 75 min post-injection, average SUL_{max} of bone metastases increases from 7.78 at 7.5 min post-injection to 13.50 at 75 min post-injection and average SUL_{max} of primary prostate tumor increases from 7.60 at 7.5 min post-injection to 11.83 at 75 min post-injection.

Figure 6a shows the normalized average SUL_{max} in comparison to the 60 min post-injection [^{68}Ga]Ga-PSMA-11 PET/CT (15, 30, 45, and 60 min). The normalized average SUL_{max} of the combined lesions at 15, 30, and, 45 min post-injection scans were all significant $p < 0.01$ different from the 60 min post-injection [^{68}Ga]Ga-PSMA-11 PET/CT (Figure 6a).
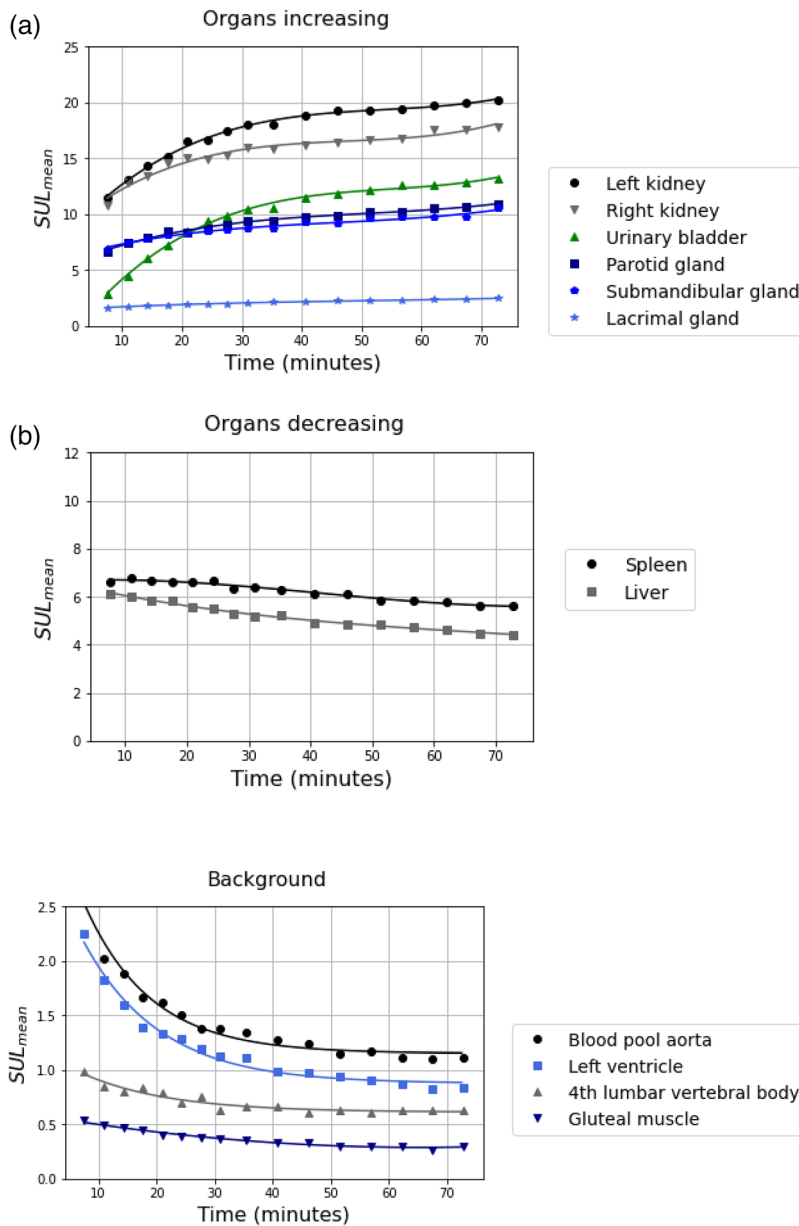
(a)

(b)

FIGURE 3 Normal organ time-activity curves over frame time. (a) increasing average standardized uptake value corrected for lean body mass (SUL$_{mean}$) over time, (b) decreasing average SUL$_{mean}$ over time. Each dot represents the mid-time of a frame.

FIGURE 4 Average mean standardized uptake value corrected for lean body mass (SUL$_{mean}$) of different background tissue over frame time. Each dot represents the mid-time of a frame.

3.4 | TBR

The gradual increase in lesion activity and decrease in background activity resulted in an increase in average TBR for lymph node metastases, bone metastases, and primary prostate tumor over time (Figure 5b).

Based on the fit average TBR of lymph nodes increases from 3.57 at 7.5 min post-injection to 13.33 at 75 min post-injection, average TBR of bone metastases increases from 9.34 at 7.5 min post-injection to 25.20 at 75 min post-injection and average TBR of primary prostate tumor increases from 3.85 at 7.5 min post-injection to 13.98 at 75 min post-injection.

Figure 6b shows the normalized TBR in comparison to the 60 min post-injection [^{68}Ga]Ga-PSMA-11 PET/CT (15, 30, 45, and 60 min). The normalized average TBR of the combined lesions at 15, 30, and 45 min post-injection scans were all significant $p < 0.05$ different from the 60 min post-injection [^{68}Ga]Ga-PSMA-11 PET/CT (Figure 6b).

3.5 | CNR

Figure 6c shows the normalized CNR in comparison to the 60 min post-injection [^{68}Ga]Ga-PSMA-11 PET/CT (15, 30, 45, and 60 min). The normalized average CNR of the combined lesions at 15, 30, and 45 min post-injection scans were all significant $p < 0.01$ different from the 60 min post-injection [^{68}Ga]Ga-PSMA-11 PET/CT (Figure 6c).
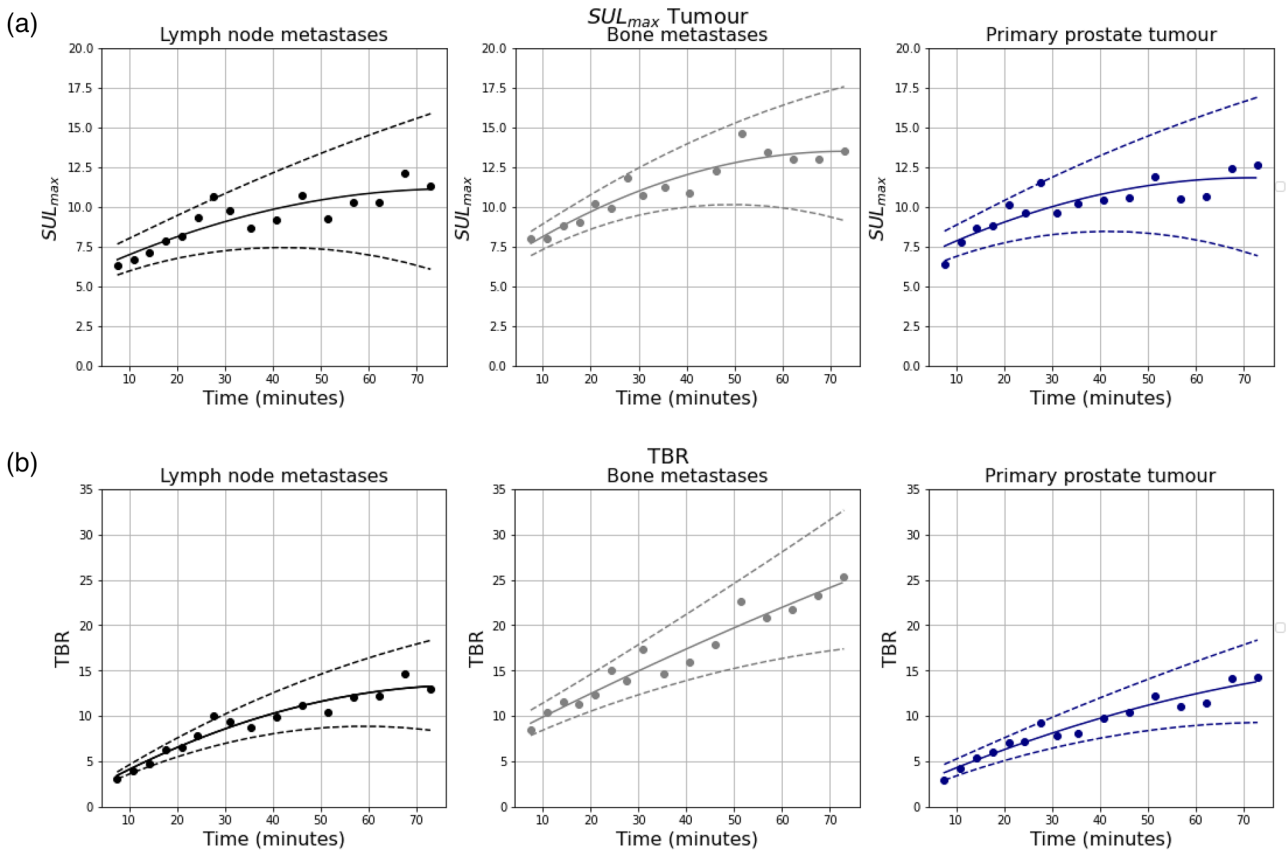
FIGURE 5 Average (a) maximum standardized uptake value corrected for lean body mass (SUL_{max}), and (b) tumor-to-background ratio (TBR) of lymph node metastases ($n = 13$), bone metastases ($n = 12$), and primary prostate tumor ($n = 6$). Each dot represents the mid-time of a frame. The solid line represents the fit, while the dashed line represents the standard deviations of the fit.

3.6 | Lesion detectability

At patient level, The reader concluded on the 60 min post-injection [^{68}Ga]Ga-PSMA-11 PET/CT (reference scan) that six patients had primary prostate cancer recurrence, five patients had lymph node metastases, and four patients bone metastases. Also the reader concluded the same regarding the present/absent of primary prostate cancer recurrence, lymph node metastases and/or bone metastases on all <60 min post-injection [^{68}Ga]Ga-PSMA-11 PET/CT's in comparison to the reference scan.

At lesion level, the reader detected 13 lymph node metastases and three bone metastases and one patient with multifocal bone metastases on the reference [^{68}Ga]Ga-PSMA-11 PET/CT. All bone metastases seen on the reference scan were also seen on all <60 min post-injection [^{68}Ga]Ga-PSMA-11 PET/CT's but there were some lymph nodes ($n = 2$) metastases missed on the 15, 30, and 45 min post-injection scans: One lymph node metastasis in one patient on both the 15 and 30 min post-injection [^{68}Ga]Ga-PSMA-11 PET/CT's (obturator loge near the right ureter) and one lymph node metastasis in another patient only on the 45 min

post-injection [^{68}Ga]Ga-PSMA-11 PET/CT (near the left intern iliac artery).

4 | DISCUSSION

Our study aimed to evaluate the possibility of a shorter time interval between [^{68}Ga]Ga-PSMA-11 administration and the start of the [^{68}Ga]Ga-PSMA-11 PET/CT acquisition by investigating the change in image quality measures by evaluating SUL_{max}, TBR, and CNR over time in 10 (metastasized) prostate cancer patients.

At 45 min, PSMA uptake (SUL_{max}) in prostate cancer lesions was already around 90% of the SUL_{max} at 60 min post-injection with high average TBR (>10) and CNR (>40). After 45 min, SUL_{max} of lesions slowly increases, and SUL_{mean} of background slowly decreased. This resulted in a continuous and gradual increase of TBR until 75 min post-injection. The CNR showed a similar pattern. The CNR percentage increase flattens off and scanning at later time points than 60 min may even increase the noise as the activity decreases, while the contrast gain is small. This effect is likely to be
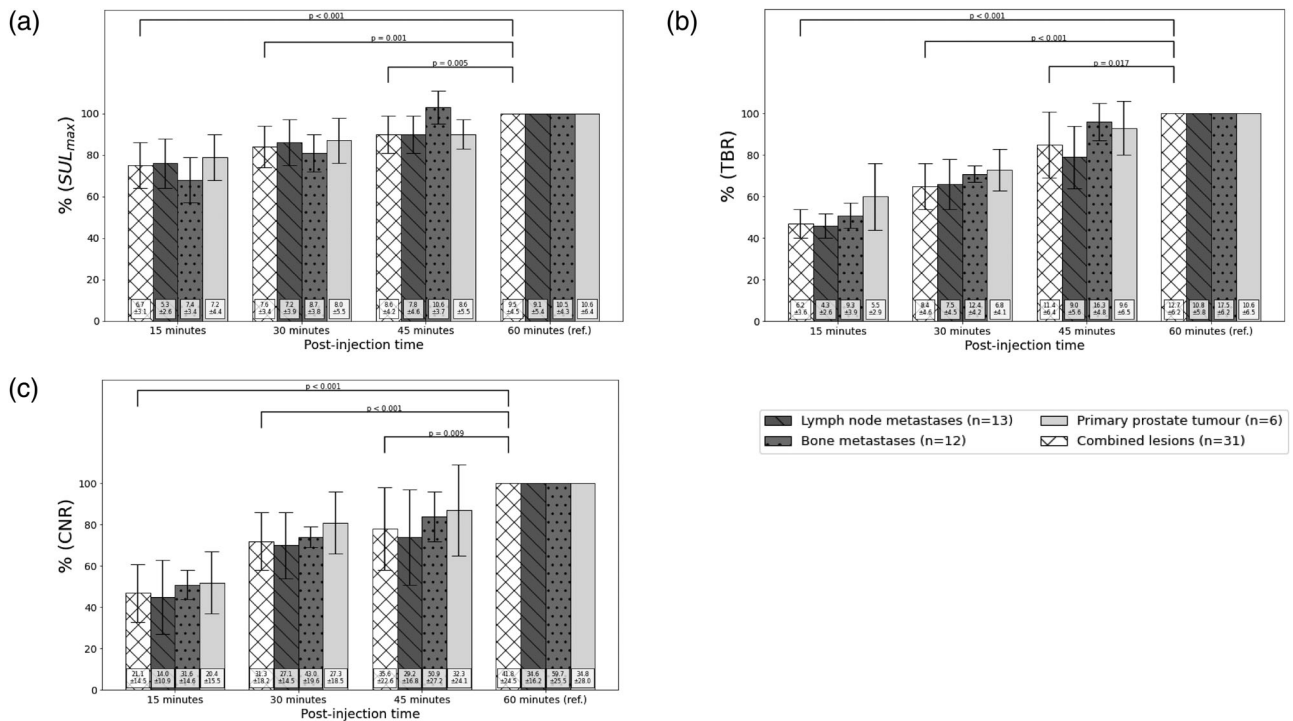
FIGURE 6 A comparison (relative) between average normalized (a) maximum standardized uptake value corrected for lean body mass (SUL_{max}), (b) tumor-to-background ratio (TBR), and (c) contrast-to-noise ratio (CNR) at 15, 30, 45, and 60 min post-injection clinical reconstructions. SUL_{max}/TBR/CNR at 60 min post-injection is taken as the reference. The average SUL_{max}/TBR/CNR value ± SD is denoted in the bar chart. Note that these values does not have to be exactly similar to the values in Figure 5 for SUL_{max} and TBR due to differences in frame duration and reconstruction. Also note that comparing the average SUL_{max}/TBR/CNR of a 15-30-45 min post-injection scan to the 60 min post-injection reference does not result in a similar % as comparing the normalized SUL_{max}/TBR/CNR.

stronger in [^{68}Ga]Ga-PSMA-11 with a half-life of 68 min than in ^{18}Fluorine (^{18}F)-labelled PSMA with a half-life of 110 min. It would therefore be interesting to investigate the time at which the optimum is reached. Though, based upon the small differences in image quality and lesion detection between 45 and 60 min, the gain after 60 min is expected to be small.

Wen et al. is the only study also evaluating the optimal uptake time of [^{68}Ga]Ga-PSMA-11 for PSMA PET/CT in 11 prostate cancer patients by performing total-body dynamic PET/CT's until 180 min post-injection.[7] Authors concluded that lesion (primary prostate tumor, lymph node metastases, and bone metastases) SUV_{mean} values were similar at 35–59 min and 60 min post-injection; however, SUV_{max}, TBR, and CNR were not reported. Our study found a significant ($p < 0.05$) negative impact on image quality measures (SUL_{max}, TBR, and CNR) when scanning earlier than 60 min post-injection. This impact became more apparent when scanning earlier than 45 min post-injection.

However, in our study, the clinical impact of earlier scanning on lesion detectability was small, no extra lesions were detected on the earlier reconstructions. At patient level, no difference was seen in the diagnosis of primary recurrence of prostate cancer and the presence/absence of lymph node and bone metastases

in all patients. SUL_{max}, TBR, and CNR did not differ much between lesion types (primary prostate tumor, lymph node- and bone metastases) at the different post-injection times (15, 30, 45, and 60 min) (Figure 6). This suggests that the impact of post-injection time is similar for different lesion types. At lesion level, two suspicious lymph node metastases on the 60 min post-injection [^{68}Ga]Ga-PSMA-11 PET/CT were missed on the 15, 30, and 45 min reconstructions.

Wen et al. additionally advised to combine conventional static imaging 60 min post-injection with early dynamic imaging (75–360 s) to avoid urinary bladder activity interference. This was also shown in the study of Uprimny et al. where all pathologic lesions within the pelvic region showed pathological [^{68}Ga]Ga-PSMA-11 uptake within the first 3 min post-injection, whereas no [^{68}Ga]Ga-PSMA-11 uptake was seen in the urinary bladder.[11] In our study no dynamic imaging was conducted of the bladder in the first 6 min after administration. However, this study did show that in early time point imaging one does have to be careful with high background activity post-injection. The TBR at 7.5 min post-injection reached only around 30% of the TBR at 60 min post-injection. This might cause low uptake lesions near the bladder difficult to distinguish in an early time frame.

Also, in our study there was some inter-reader variability between the blinded reader and the clinical report. This can be explained by the fact that the clinician had access to patients history and previous scans.

Our study chose to correct standardized uptake values (SUV) for lean body mass (SUL)[8] as SUV has a positive correlation with body weight, while SUL is not correlated to body weight. The SUL is 18%−31% lower in this patient group than the SUV value.[12] One should therefore be careful when comparing these results to SUV values of other papers. A comparison of SUV/SUL with the study of Wen et al.[7] does show the trend in SUV/SUL is similar.

Our study had several limitations: First, the sample size was small and the population heterogeneity could be improved in future studies. Second, no histological confirmation of the tumor lesions was available as it mostly concerned prostate cancer recurrences. Third, no delineation was done of the healthy prostate tissue as it was not possible to distinguish healthy tissue from prostate cancer, and only one patient with prostate in situ had no prostate cancer recurrence. Fourth, due to the acquisition protocol, the scan reconstruction at 15 min post-injection was a 9 min reconstruction (3×3 min frames), in contrast to the reconstructions after 30, 45, and 60 min that consisted of 10 min reconstructions (2×5 min frames).

Finally, it should be noted that in the dynamic analysis of the SUL_{max} and TBR, time points referred to were mid-frame times, while in the clinical reconstruction analysis the referred time was the start of the scan.

As our study analyzed the results in a group of 10 patients, it would be recommended to do further research on lesion detection with a larger patient group.

5 | CONCLUSIONS

Image quality measures SUL_{max}, TBR, and CNR all increases with longer post-injection times. Therefore, shorter post-injection times (15, 30, and 45 min) compared to the recommended post-injection time of 60 min are not optimal. However, the impact of a shorter time interval of 45 min instead of 60 min between [^{68}Ga]Ga-PSMA-11 administration and the start of PET/CT acquisition on both image quality and lesion detection, while significant, is small.

ORCID
Esmée C. A. van der Sar
https://orcid.org/0000-0003-4406-2409
Sebastiaan L. Meyer Viol
https://orcid.org/0000-0001-5559-9012
Arthur J. A. T. Braat
https://orcid.org/0000-0002-8824-8697
Rob van Rooij
https://orcid.org/0000-0001-8546-8283
Marnix G. E. H. Lam
https://orcid.org/0000-0002-4902-9790
Hugo W. A. M. de Jong
https://orcid.org/0000-0002-3000-8316
Bart de Keizer
https://orcid.org/0000-0002-6270-9483

REFERENCES

1. van Kalmthout LWM, van Melick HHE, Lavalaye J, et al. Prospective validation of gallium-68 prostate specific membrane antigen-positron emission tomography/computerized tomography for primary staging of prostate cancer. *J Urol.* 2020;203(3):537-545. doi:10.1097/JU.0000000000000531

2. Jansen BHE, Kramer GM, Cysouw MCF, et al. Healthy tissue uptake of (68)Ga-prostate-specific membrane antigen, (18)F-DCFPyL, (18)F-fluoromethylcholine, and (18)F-dihydrotestosterone. *J Nucl Med.* 2019;60(8):1111-1117. doi:10.2967/jnumed.118.222505

3. Afshar-Oromieh A, Holland-Letz T, Giesel FL, et al. Diagnostic performance of (68)Ga-PSMA-11 (HBED-CC) PET/CT in patients with recurrent prostate cancer: evaluation in 1007 patients. *Eur J Nucl Med Mol Imaging.* 2017;44(8):1258-1268. doi:10.1007/s00259-017-3711-7

4. European Association of Urology. EAU-EANM-ESTRO-ESUR-SIOG Guidelines on Prostate Cancer 2020. [Internet]. Accessed April 2020. https://uroweb.org/guideline/prostate-cancer/

5. Fendler WP, Eiber M, Beheshti M, et al. (68)Ga-PSMA PET/CT: joint EANM and SNMMI procedure guideline for prostate cancer imaging: version 1.0. *Eur J Nucl Med Mol Imaging.* 2017;44(6):1014-1024. doi:10.1007/s00259-017-3670-z

6. Afshar-Oromieh A, Malcher A, Eder M, et al. PET imaging with a [68Ga]gallium-labelled PSMA ligand for the diagnosis of prostate cancer: biodistribution in humans and first evaluation of tumour lesions. *Eur J Nucl Med Mol Imaging.* 2013;40(4):486-495. doi:10.1007/s00259-012-2298-2

7. Wen J, Zhu Y, Li L, Liu J, Chen Y, Chen R. Determination of optimal (68) Ga-PSMA PET/CT imaging time in prostate

cancers by total-body dynamic PET/CT. *Eur J Nucl Med Mol Imaging*. 2021;49:2086-2095. doi:10.1007/s00259-021-05659-8

8. Janmahasatian S, Duffull SB, Ash S, Ward LC, Byrne NM, Green B. Quantification of lean bodyweight. *Clin Pharmacokinet*. 2005;44(10):1051-1065. doi:10.2165/00003088-200544100-00004

9. Gafita A, Calais J, Franz C, et al. Evaluation of SUV normalized by lean body mass (SUL) in (68)Ga-PSMA11 PET/CT: a bi-centric analysis. *EJNMMI Res*. 2019;9(1):103. doi:10.1186/s13550-019-0572-z

10. Wielaard J, Habraken JBA, Brinks P, Lavalaye J, Boellaard R. Optimization of injected (68)Ga-PSMA activity based on list-mode phantom data and clinical validation. *EJNMMI Phys*. 2020;7(1):20. doi:10.1186/s40658-020-00289-9

11. Uprimny C, Kroiss AS, Decristoforo C, et al. Early dynamic imaging in (68)Ga- PSMA-11 PET/CT allows discrimination of urinary bladder activity and prostate cancer lesions. *Eur J Nucl Med Mol Imaging*. 2017;44(5):765-775. doi:10.1007/s00259-016-3578-z

12. Aksu A, Capa Kaya G. Is SUV corrected for lean body mass superior to SUV of body weight in (68)Ga-PSMA PET/CT? *Mol Imaging Radionucl Ther*. 2021;30(3):144-149. doi:10.4274/mirt.galenos.2021.59254

How to cite this article: van der Sar ECA, Viol SLM, Braat AJAT, et al. Impact of uptake time on image quality of [68Ga]Ga-PSMA-11 PET/CT. *Med Phys*. 2023;50:7619–7628. https://doi.org/10.1002/mp.16429